A simulation study of pearlite-to-austenite transformation kinetics in rapidly heated hot-rolled low carbon steel

Article *in* Materials & design · October 2016

DOI: 10.1016/j.matdes.2016.06.025

CITATIONS
3

READS
334

5 authors, including:

Sandeep Sharma
Thapar University
2 PUBLICATIONS **4** CITATIONS
SEE PROFILE

Tarun Nanda
Thapar University
31 PUBLICATIONS **32** CITATIONS
SEE PROFILE

Venugopalan Thirumalachari
Tata Steel Limited, India
43 PUBLICATIONS **131** CITATIONS
SEE PROFILE

B. Ravi Kumar
National Metallurgical Laboratory
91 PUBLICATIONS **1,243** CITATIONS
SEE PROFILE

Materials and Design 107 (2016) 65–73

Contents lists available at ScienceDirect

Materials and Design

journal homepage: www.elsevier.com/locate/matdes

A simulation study of pearlite-to-austenite transformation kinetics in rapidly heated hot-rolled low carbon steel

Sandeep Sharma [a], Tarun Nanda [a,*], Manashi Adhikary [b], T. Venugopalan [b], B. Ravi Kumar [c]

[a] Mechanical Engineering Department, Thapar University, Patiala 147004, India
[b] Tata Steel Limited, Jamshedpur 831001, India
[c] CSIR-National Metallurgical Laboratory, Jamshedpur 831007, India

ARTICLE INFO

Article history:
Received 21 March 2016
Received in revised form 15 May 2016
Accepted 7 June 2016
Available online 08 June 2016

Keywords:
DICTRA
Simulation
Kinetics
Rapid heating
Dual-phase
Continuous annealing

ABSTRACT

The main aim of the present research was to obtain an optimized microstructure with adequate mechanical properties in a low carbon steel. The effect of microstructure on kinetics of austenite transformation was simulated. A 3.2 mm hot rolled steel was subjected to continuous annealing to obtain properties of Dual Phase 590 grade. Kinetics of austenite transformation was studied with respect to the condition of just pearlite dissolution to form austenite under rapid heating. Annealing parameters were based on process conditions of dual phase steel production in a continuous annealing line. DICTRA was used to simulate heating rates of the order 10–500 °C/s with peak temperatures in the range 750–850 °C to predict isothermal annealing time required for complete dissolution of pearlite into austenite under different temperature-heating rate conditions. Simulation results showed dependency of temperature and heating rate on austenite transformation time. Interestingly, no significant effect of heating rate on complete pearlite dissolution into austenite was evident. Results were validated with limited experimentation on Gleeble. Microstructure analysis validated the simulation results to be accurate. The observations have pertinent inputs while designing industrial continuous annealing line parameters where rapid heating rates are generally encountered (10–20 °C/s).

1. Introduction

Dual phase (DP) steels have proved a great potential in automobile sector for better fuel economy and passenger safety because of their superior specific strength [1–5]. DP steels consist of polygonal ferrite and martensite/bainite phases [6,7]. Ferrite phase is responsible for ductility whereas martensite/bainite phase is responsible for strength [8–10]. A good combination of strength and ductility can be obtained by achieving proper distribution of both the phases. The strength of DP steel depends upon the martensite volume fraction (MVF), the carbon content in martensite which determines its hardness, and the distribution of martensite phase in the microstructure [11–15]. Therefore, carbon dissolution in austenite during annealing is a critical parameter. The carbon content in austenite is maximum if austenite formation occurs just simultaneously with pearlite dissolution [16–18]. Austenite formation in the inter-critical region has been extensively studied [19–21]. Austenite growth in the given steel can be controlled by controlling the carbon diffusion in ferrite [22]. Austenite formation takes place in three basic steps: dissolution of pearlite into austenite (Step-I), growth of austenite into pro-eutectoid ferrite (Step-II), homogenization of the austenite formed (Step-III) [23]. The austenite formed during Step-I has maximum carbon concentration. With Step-II and Step-III, the volume fraction of austenite increases but carbon concentration in austenite decreases [16]. Austenite formed in Step-I has maximum carbon concentration, and further, the time required for formation of such austenite is minimum [17]. Thus, the holding time required for just pearlite dissolution into austenite assumes a critical importance for determining martensite fraction and hardness. From an industrial viewpoint, rapid heating rates are required for dual phase steel processing by continuous annealing line for meeting the objective of high production rates, reduced processing time, and increased annealing cycle efficiency. To fulfil these objectives, it is necessary that the important annealing parameters viz. heating rates, annealing temperatures, isothermal holding time periods, etc. be simulated [2,24]. In the present work, simulations were conducted on DICTRA software (Diffusion Controlled TRAnsformations software; DICTRA: version 27; developed by Thermo-Calc Software AB, Stockholm, Sweden) to determine the isothermal annealing time for complete pearlite dissolution into austenite at given annealing temperature-heating rate combinations. For DICTRA simulations, the local equilibrium model predicts the fraction of austenite/ferrite most accurately [25], and therefore, the local equilibrium model was used in

* Corresponding author.
E-mail addresses: sandeep54909@gmail.com (S. Sharma), tarunnanda@thapar.edu, ananda@thapar.edu (T. Nanda), manashia@gmail.com (M. Adhikary), ravik@nmlindia.org (R.K. B.).

http://dx.doi.org/10.1016/j.matdes.2016.06.025
0264-1275/

Table 1
Chemical composition of the *as*-received hot rolled steel.

Element	C	Mn	Si	S	P	Al	N	Fe
% wt.	0.074	1.83	0.43	0.002	0.012	0.026	0.0032	Balance

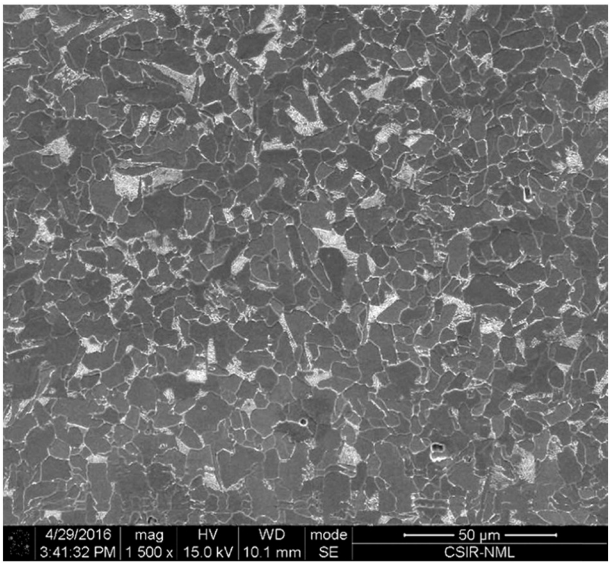

Fig. 1. Microstructure of the as-received hot rolled steel showing typical hot rolled structure consisting of ferrite and pearlite.

the current investigations. In the local equilibrium model, the interface is assumed to migrate under full local equilibrium conditions with both partitioning of carbon and alloying elements [25,26]. The present work is an attempt to simulate the rapid heating rates during continuous annealing and to investigate their impact on pearlite dissolution into austenite. DICTRA simulations were validated through experimental Gleeble simulations.

2. Experimental

2.1. Characterization of the as-received material

Experiments were performed on an industrially hot rolled steel sheet having chemical composition as shown in Table 1.

Specimens were subjected to standard metallographic procedure and were etched using nital (for normal etching; 2% nital solution) and picral reagent (for color etching; pre-etched in 0.4 g picric acid in 10 ml ethanol for 60 s and finally etched in solution of 1 g sodium metabisulphate in 10 ml distilled water) for optical microscopy. Picral being a color etchant showed martensite as dark brown and ferrite as white. A Leica microscope (DM2500 M) of Lieca Microsystems, Germany was used. For SEM microscopy, a scanning electron microscope set-up (Nova Nano SEM 430; Field Emission Inc., Hillsboro, USA) was used. Phase fractions in the microstructure and grain size distribution were determined using 'analySIS FIVE' software (analySIS Five 5.05.07; developed by Olympus Soft Imaging Solutions, Notting Hill, Australia). Finally, tensile tests were performed as per ASTM standard E–8 M at room temperature. Tests were conducted using flat dog-bone shaped specimens of 25 mm gauge length, strain rate of 1×10^{-3} $s^{-}1$ on an Instron 8862 system with 100 kN capacity.

The microstructure of the starting material typically comprised of ferrite and pearlite as shown in Fig. 1. By using the linear intercept method, the average grain size was determined as 9.13 µm. The volume fraction of pearlite was calculated as 18.82% using 'analySIS FIVE' software.

3. Predictions of phase fraction using Thermo-Calc

The inter-critical annealing temperature range for the given steel chemistry was determined using Thermo-Calc (Thermo-Calc 3.0; Thermo-Calc Software AB, Stockholm, Sweden). The predicted phase diagram is shown in Fig. 2. Lower (Ac_1) and upper (Ac_3) critical temperatures were predicted as 676 °C and 839 °C respectively as shown in Fig. 2(a). Fig. 2(b), shows the predicted phase fraction or increase in the volume fraction of austenite with increase in inter-critical (lower (Ac_1) and upper (Ac_3)) annealing temperatures under equilibrium conditions.

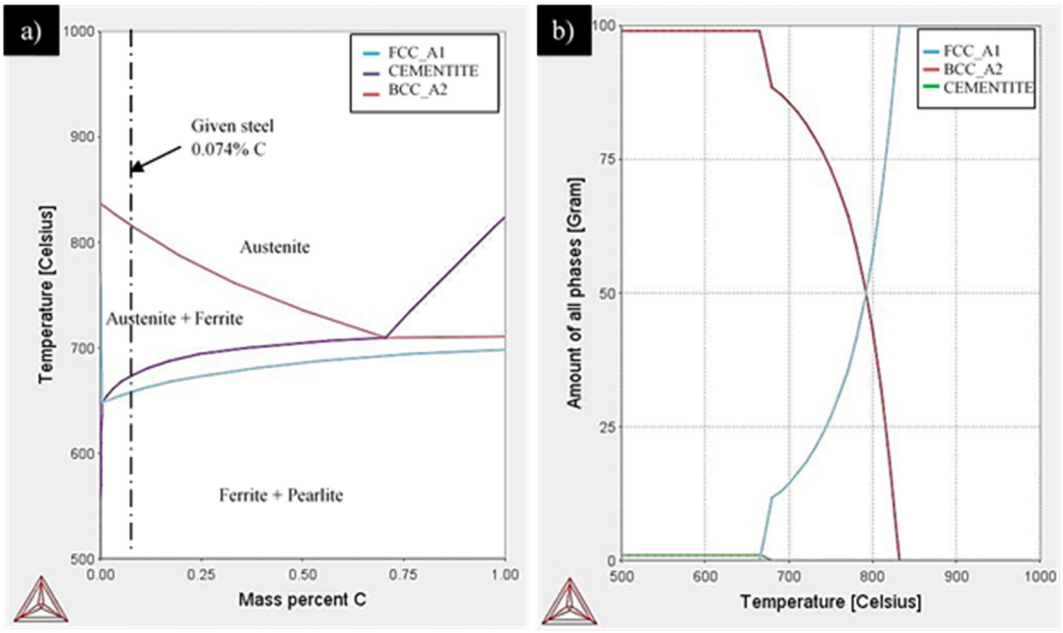

Fig. 2. Result window of Thermo-Calc for (a) phase diagram (b) change in volume fraction of various phases within inter-critical annealing temperature range under equilibrium conditions.

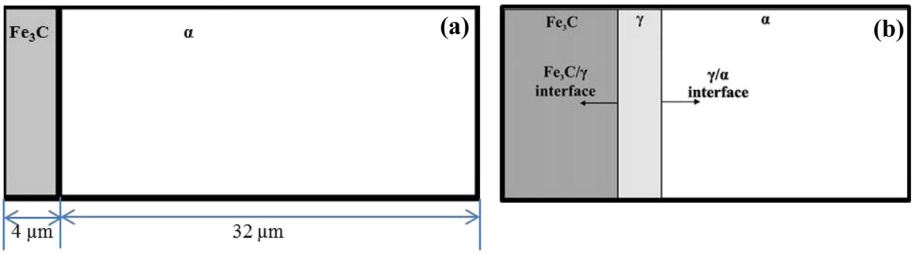

Fig. 3. Representation of the lamellar pearlite assumed for simulation (a) the initial state of pearlite, and (b) formation of austenite by dissolution of pearlite.

4. Predictions of complete pearlite dissolution using DICTRA

DICTRA was used to understand the pearlite dissolution behavior in the inter-critical annealing temperature range. For the steel under investigation, the lower critical temperature was predicted as 676 °C by using Thermo-Calc. However, DICTRA simulations were carried out for inter-critical annealing temperature range between 750 and 850 °C , with temperature intervals of 25 °C. Inter-critical temperatures lower than 750 °C were not considered for the detailed simulations because soaking time periods required for complete pearlite dissolution into available austenite fraction for these temperatures (between 676 and 750 °C) were extremely high. For example, for annealing temperature of 750 °C , the soaking time for complete pearlite dissolution provided by DICTRA was about 1038 s which was extremely high as compared to time periods utilized in industrial continuous annealing lines. Thus, from a practical industrial annealing viewpoint, the actual inter-critical range was considered as 750–850 °C .

Further, for simulation work, the pearlite shape was assumed to be completely lamellar. A linear system, with ferrite and cementite in the ratio of 8:1 was chosen with interfacial regions Fe_3C/γ and γ/α as shown in Fig. 3a–b. This ratio was arrived at from measurements on the as-received hot rolled pearlite structure. A typical inter-lamellar spacing at high magnification is shown in Fig. 4. Further, for the purpose of simulation, one dimensional geometry was used with system size of 36 μm (see Fig. 3a). In Fig. 3a, the initial distance of 4 μm (from 0–4 μm on X-axis) is representing cementite lamella and the remaining distance of 32 μm (from 4–36 μm) is representing ferrite lamella. Fig. 3b demonstrates the growth of austenite into both cementite (0–4 μm region) and ferrite (4–32 μm region) lamella.

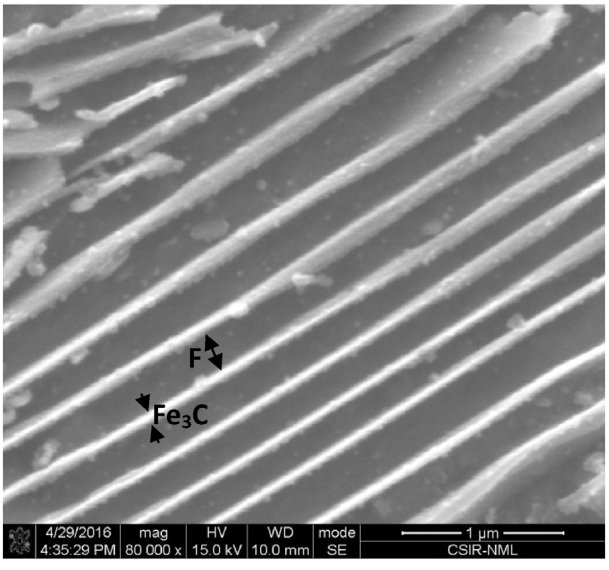

Fig. 4. SEM microstructure showing inter-lamellar ferrite–cementite width in pearlite. F = ferrite, Fe_3C = cementite.

In this study, only pearlite dissolution and its transformation to austenite was modelled during heating to different annealing temperatures at various heating rates. It may also be noted that simulation results predicted the austenite volume fraction obtained as a result of pearlite dissolution and not the total volume fraction of austenite in the microstructure. Simulation was carried out in two phases. Phase-I investigated the effect of heating rates (10, 20, 50, 100, 200, 300, 400, 500 °C/s) used in reaching the isothermal annealing temperature on pearlite dissolution. In Phase-II, the combined effect of heating rate and isothermal annealing time on just completion of pearlite dissolution was evaluated. For Phase-I simulations, the initial state of the system was considered to be at room temperature of 27 °C. Transformation or dissolution of pearlite via austenite-ferrite lamella formation was considered as the primary mechanism in case of DICTRA simulations. Three discreet transformation steps were simulated during heating; a) austenite nucleation at cementite-ferrite interface in no time, b) diffusion of carbon into austenite from cementite and c) growth of austenite into ferrite to attain equilibrium state [19]. Hence, as the transformation would progress, the width of austenite region adjacent to original cementite lamella (i.e. adjacent to cementite-austenite interface) would grow. Therefore, pearlite transforms into austenite-ferrite lamella. A typical simulation output of Phase–I at different heating rates to attain annealing temperature of 800 °C is shown in Fig. 5. Fig. 5(a–h) presents the results of DICTRA simulations showing change in carbon concentration in the growing austenite phase at different heating rates at 800 °C . It can be noted that austenite formed (from pearlite dissolution) at a given heating rate-annealing temperature combination is not of uniform composition. Austenite formed has a varying chemical composition with more carbon in austenite towards the Fe_3C/γ interface and less carbon content towards the γ/α interface. Fig. 5 shows the variation in chemical composition of freshly formed austenite phase. For example, Fig. 5a shows the carbon percent in austenite to be varying between 0.9% carbon to 0.3% carbon. This variation in chemical composition of austenite from Fe_3C/γ interface towards γ/α interface is an experimentally observed fact and is well reported in literature also [27–29]. Therefore, diffusion distance is a representative of extent of carbon heterogeneity in austenite before its equilibration with ferrite (Fig. 5a). Further, it can be noted from Fig. 5(a–h) that at a given simulation temperature (here 800 °C), as the heating rate increases, the amount of austenite fraction formed decreases.

In the DICTRA result window (Fig. 5a), austenite formation is represented by region where slope changes continuously. It can be noted that slope starts to change at point A (at distance slightly less than 4 μm) and ends changing at point B (about 9 μm). Thus, Fig. 5a indicates that for the distance from 0 to slightly less than 4 μm (on X-axis), cementite phase is still present (initially when steel was at room temperature, cementite extended from 0 to 4 μm) and for the distance from about 9 μm to 36 μm (on X-axis), ferrite phase is still present. However, for the distance between 4 to 9 μm (where slope is continuously changing), the newly formed austenite phase is present because of pearlite dissolution. Thus, for this heating rate and annealing temperature combination, austenite amount formed corresponds to distance ranging from 4–9 μm. For a change in heating rate at a given annealing temperature, if this distance (over which slope continuously changes) increases, the austenite

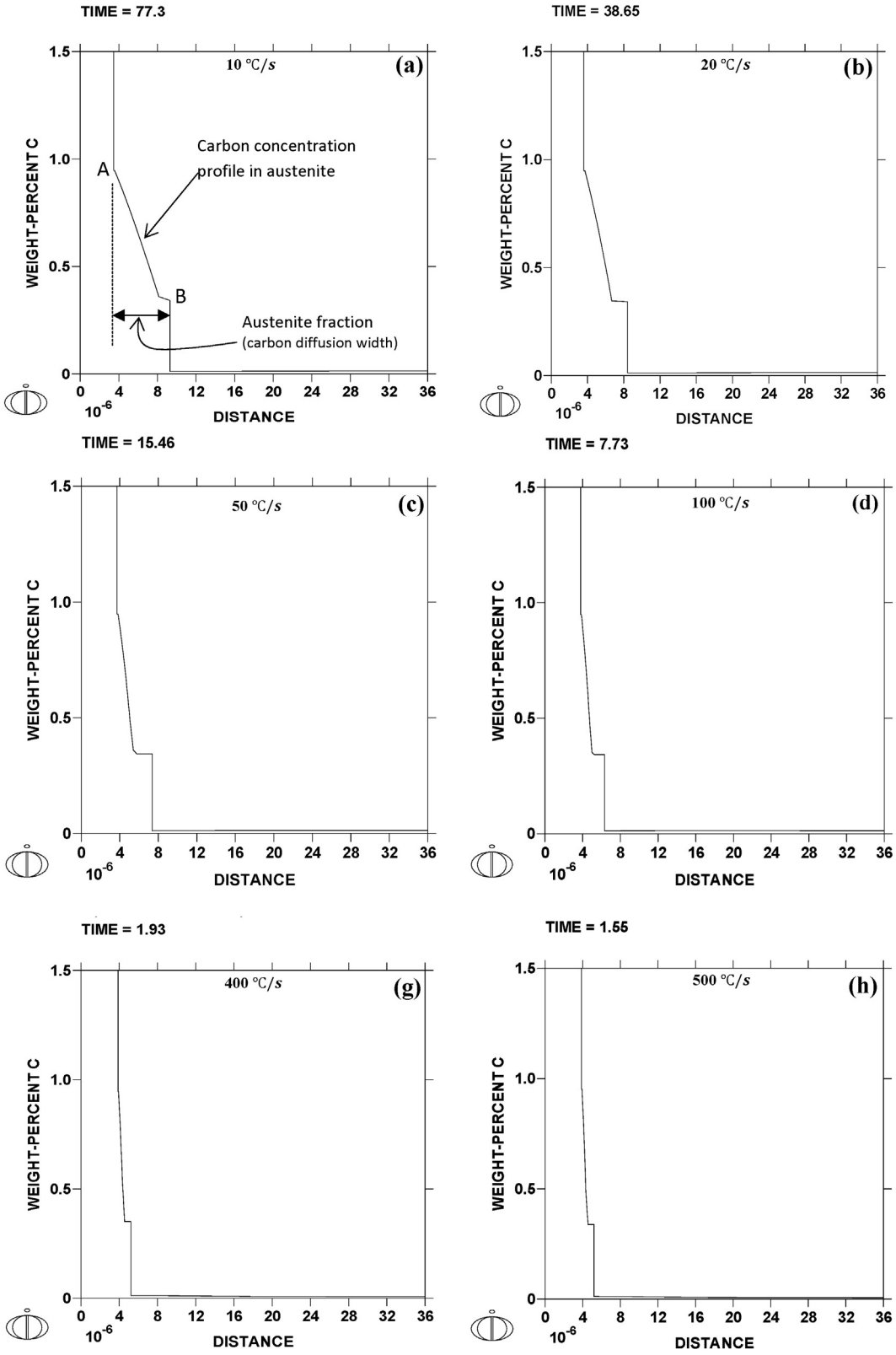

Fig. 5. Result of DICTRA simulations showing carbon concentration profile in austenite, at different heating rates at the given annealing temperature of 800 °C (a) 10 °C/s, (b) 20 °C/s, (c) 50 °C/s, (d) 100 °C/s, (e) 200 °C/s, (f) 300 °C/s, (g) 400 °C/s, and (h) 500 °C/s. DISTANCE = distance from the starting cementite lamella interface into austenite, in microns.

amount would increase and vice-versa. It can be noted that at the given temperature of 800 °C, as the heating rate increases, the distance (over which slope continuously changes) decreases and hence amount of austenite fraction formed decreases. Thus, increase in heating rate decreases the volume fraction of austenite formed or retards pearlite dissolution. This is because, as the heating rate increases, the time required for reaching the isothermal annealing temperature decreases, and thus, the progress of diffusion controlled austenite phase transformation process slows down. Table 2 presents the results with regards to fraction of austenite obtained through pearlite dissolution at different

Table 2
Effect of heating rate and annealing temperature on the austenite fraction obtained through pearlite dissolution.

Heating rate (°C/s)	Austenite fraction obtained through pearlite dissolution				
	750 °C	775 °C	800 °C	825 °C	850 °C
10	1.83	9.25	16.27	25.50	37.80
20	1.22	4.94	13.55	21.22	29.81
50	1.22	3.39	10.47	18.60	25.20
100	0.92	2.44	7.06	13.56	19.06
200	0.88	2.44	5.83	9.83	14.75
300	0.94	2.14	4.61	8.00	9.22
400	0.94	1.83	4.00	7.69	8.94
500	0.02	1.83	4.00	6.75	7.69

Table 3
Critical isothermal annealing time required for just completion of pearlite dissolution.

Heating rate (°C/s)	Holding time period[a] (s) at annealing temperature (Phase-II Simulations) of				
	750 °C	775 °C	800 °C	825 °C	850 °C
10	1038	327	141	67	32
20	1043	328	142	68	33
50	1043	330	143	67	31
100	1043	329	144	70	36
200	1043	331	144	71	37
300	1043	330	144	71	38
400	1043	330	144	71	38
500	1043	330	144	71	38

[a] Holding time required at a given annealing temperature for complete (100%) dissolution of just pearlite into austenite.

combinations of heating rate-annealing temperature conditions. As expected, the austenite fraction obtained through pearlite dissolution was found to increase with increase in inter-critical annealing temperature. Further, it may also be noted from the results that residual fraction of pearlite increased with increase in heating rate at a given annealing temperature.

It can be observed from Table 2 that for a given annealing temperature, the heating rate plays a vital role in pearlite dissolution for austenite formation. For a specific annealing temperature, with increase in heating rate, the fraction of pearlite transforming into austenite, decreases [30]. The effect of heating rate and annealing temperature on austenite formation is presented in Fig. 6. Fraction of austenite formed for any given heating rate increases with annealing temperature.

The results of Phase-I simulations were used as input data for Phase-II simulations. Table 3 presents the results of Phase-II simulations providing soaking time periods required for completion of just pearlite dissolution into austenite at a given heating rate-annealing temperature combination. It can be observed that holding time required for complete pearlite dissolution at a given annealing temperature is not significantly affected by change in heating rate.

5. Results and discussion

To validate simulation predictions, annealing experiments for some selected processing conditions were performed on Gleeble 3800 simulator (Make: Dynamic System Inc., Poestenkill, New York, USA).

Experiments were conducted to meet three main objectives:

(i) to validate the inter-critical annealing temperature range obtained through Thermo-Calc and to confirm that the heating rates chosen for DICTRA simulations were capable of initiating pearlite dissolution into austenite without isothermal annealing. For the first objective, annealing experiments were performed at a constant heating rate of 20 °C/s, wherein detectable pearlite dissolution was predicted (Table 2), at all the annealing temperatures (see Fig. 7). The corresponding microstructures are shown in Fig. 8.

(ii) To validate the holding time required for just pearlite dissolution predicted by DICTRA simulations under different heating rate-annealing temperature combinations. For this, annealing experiments were performed with heating rate of 20 °C/s at two annealing temperatures of 800 and 825 °C (see Figs. 9–10). It may be noted that since the predicted time required for just pearlite dissolution at annealing temperature of 750 °C was quite high (1038 s, which is not suitable for industrial applications; see Table 3), hence it was not considered.

(iii) To investigate the mechanical properties obtained in the given steel subjected to different annealing temperatures under various heating rate-isothermal annealing time combinations. The main objective of this was to validate the presumption that presence of carbon rich martensite (obtained from carbon rich austenite formed through just pearlite dissolution) in DP steel results in enhanced strength and ductility. For the third objective, tensile test was conducted at a heating rate of 10 °C/s for annealing temperature of 850 °C. With these parameters it was possible to achieve just pearlite dissolution with reasonable fraction of martensite at a shortest possible process time (Table 3).

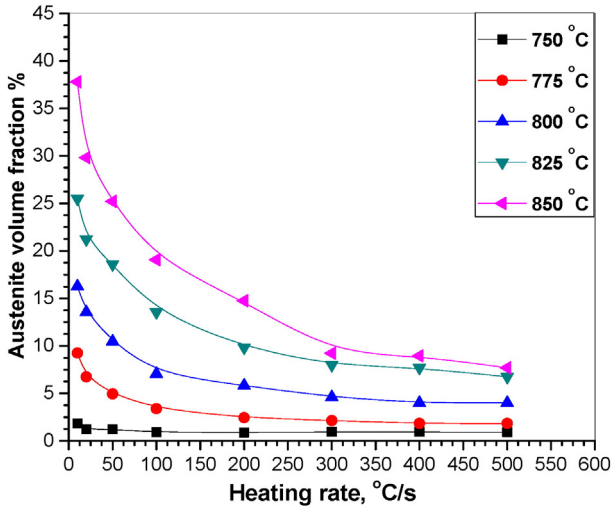

Fig. 6. DICTRA simulation results showing effect of annealing temperature and heating rate on austenite volume fraction.

Fig. 7 presents the time-temperature profiles obtained through Gleeble simulations for various annealing temperatures at heating rate of 20 °C/s.

After the Gleeble experiments for various annealing temperatures at heating rate of 20 °C/s, all specimens were analyzed by SEM microstructure studies for confirmation of the onset of pearlite dissolution. Fig. 8 shows the SEM micrographs depicting progress of pearlite dissolution and the consequent austenitic phase formation with increase in temperature. Austenite formation was indirectly evidenced through formation of martensite due to rapid cooling of specimen after heating. Microstructure analysis showed the presence of partially dissolved pearlite at all annealing temperatures and the extent of dissolution increased with temperature. Further, Fig. 8(d) supports our model assumption of austenite growth front parallel to cementite-ferrite lamella which results in transformation of ferrite-cementite lamella into ferrite-austenite lamella. Therefore, shape and orientation of martensite laths assumes from shape and orientation of lamellar ferrite-austenite structure because partially growing austenite lath transforms to martensite lath during rapid cooling. It is important to note here that under equilibrium conditions, after completion of pearlite dissolution, carbon enriched austenite grows into adjacent ferrite to achieve equilibrium

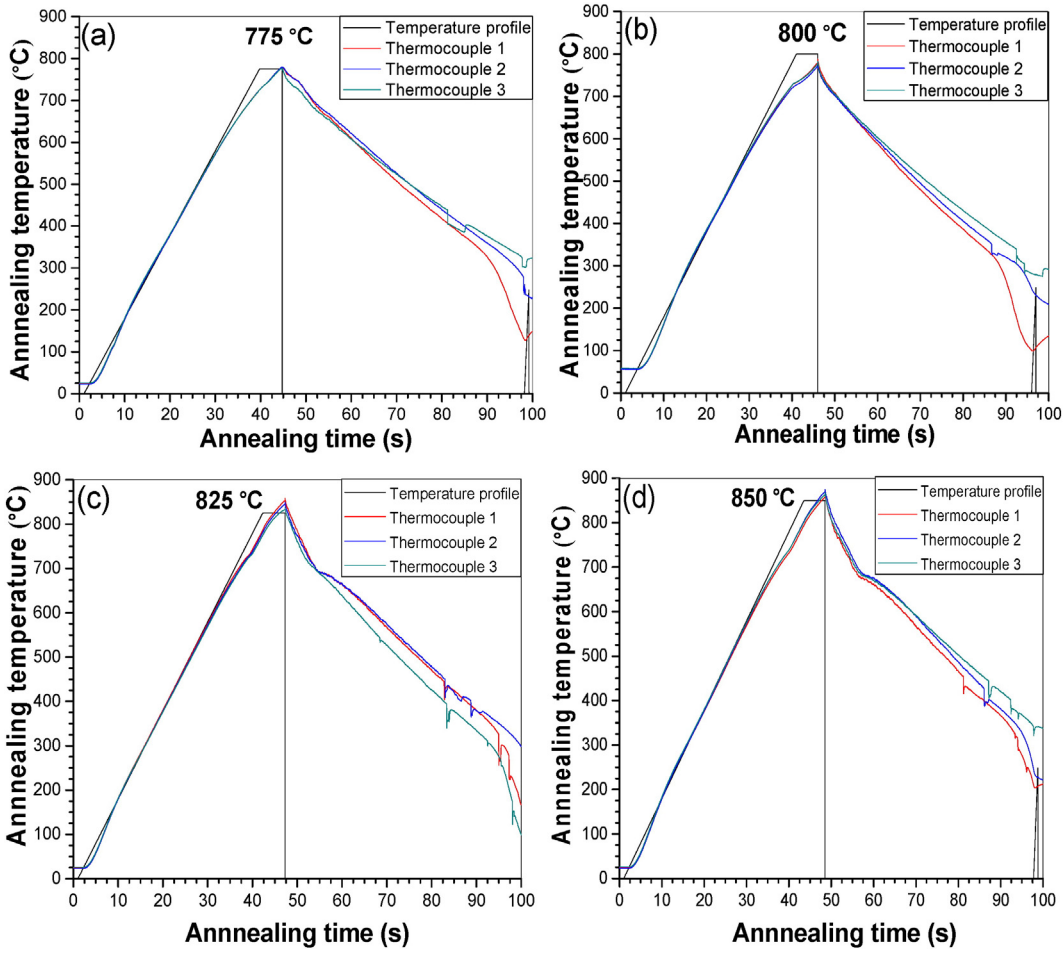

Fig. 7. Time-temperature profiles at a constant heating rate of 20 °C/s for annealing temperature of (a) 775, (b) 800, (c) 825, and (d) 850 °C.

and in the process takes polygonal grain shape. In this case, martensite morphology would be different.

The presence of martensite in the microstructure at all the annealing temperatures confirmed that the onset of pearlite dissolution or austenite transformation occurred. This validated that the inter-critical temperature range predicted by Thermo-Calc software and the heating rate (of 20 °C/s) chosen for the study were correct.

Phase-II DICTRA simulations to predict the holding time required for just pearlite dissolution into austenite were validated by Gleeble experiments. Experiments were conducted for the heating rate of 20 °C/s for two annealing temperatures of 800 °C and 825 °C. The isothermal holding time periods for 800 °C and 825 °C were 142 s and 68 s respectively (as were predicted by DICTRA simulations; see Table 3). After completion of annealing, specimens were water quenched. Fig. 9 shows the typical time-temperature profiles generated by Gleeble simulation.

FEG-SEM micrographs, as shown in Fig. 10, revealed presence of ferrite and martensite in the microstructure, with little or no residual pearlite. This showed that for the given isothermal annealing time-temperature combinations complete dissolution of pearlite to austenite had occurred, thus validating predictions of soaking period. Also, phase fraction measurements (through 'analySIS FIVE' software) provided martensite volume fractions at the two annealing temperature as about 19.61% and 20.15% respectively. These amounts matched closely with the initial pearlite content (18.82%) in the as-received steel, thus further validating the simulation results i.e. austenite formation was just through pearlite dissolution. The experimental results and the Phase-II simulation predictions were in close agreement, thereby validating the latter to be accurate.

5.1. Evaluation of tensile properties

The simulation results revealed that the shortest holding time for complete pearlite dissolution (i.e. maximum austenite and hence martensite fraction without any residual pearlite) was about 32 s at annealing temperature of 850 °C. To evaluate the possible increase in tensile properties at such short possible soaking time, tensile test was conducted on the specimen processed with heating rate of 10 °C/s at 850 °C. The specimen was heated to the desired annealing temperature of 850 °C following a heating rate of 10 °C/s, and held for a soaking periods of 32 s. After completion of the annealing cycle, the specimen was rapidly cooled to room temperature. Fig. 11a–b shows the time-temperature profile and the typical micrograph of steel specimen annealed under the above condition.

The color etched micrograph of the specimen under the given annealing condition (Fig. 11b) clearly shows a dual phase microstructure comprising of ferrite and martensite phases. Further, the martensite area fraction (19.80%) in the microstructure under the given condition is in agreement with the pearlite fraction (18.82%) in the as-received state. This shows that the experimental results are in complete agreement with the simulation results. Thus, the holding time periods as predicted by DICTRA simulations are well suited in attaining the carbon rich austenite (i.e. austenite formed as a result of pearlite dissolution only) in the given steel.

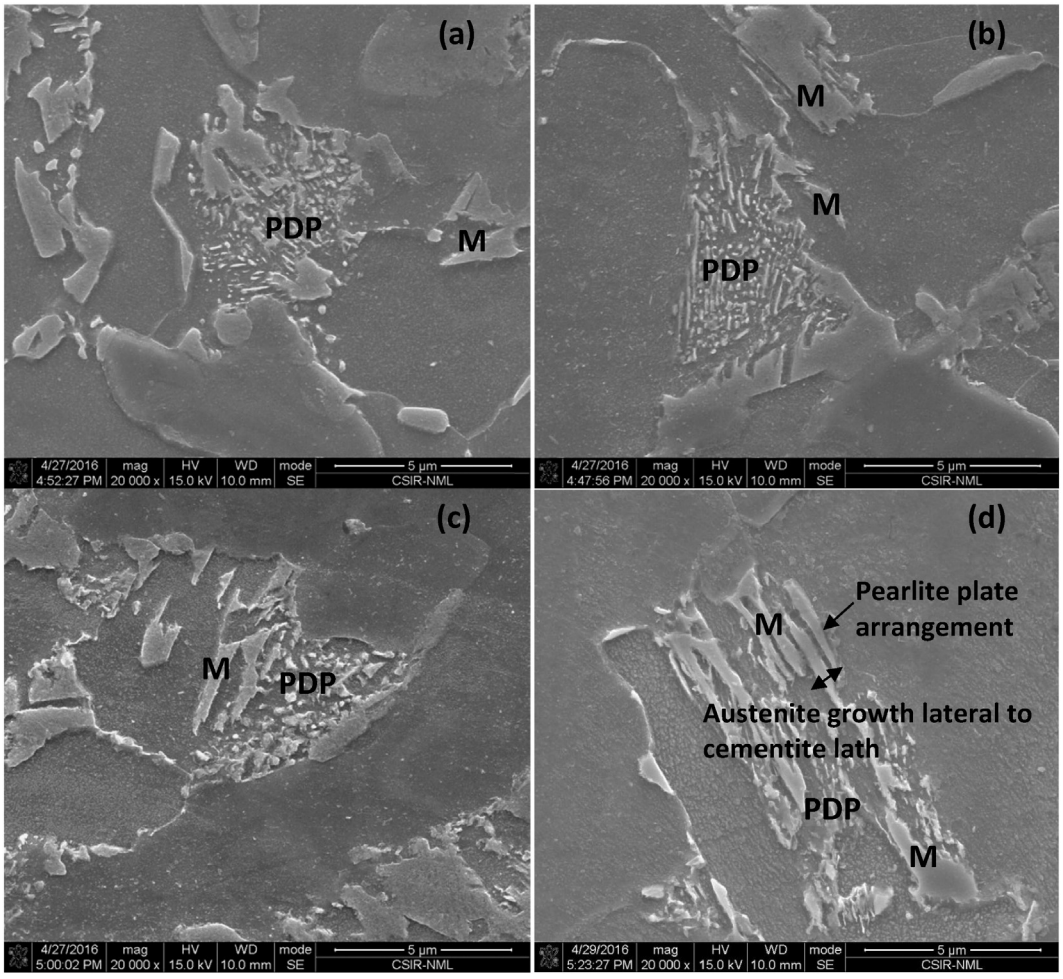

Fig. 8. FEG-SEM micrographs of specimens subjected to heating rate of 20 °C/s for annealing temperatures of (a) 775 °C, (b) 800 °C, (c) 825 °C and (d) 850 °C. Some of these phases are identified in the micrographs by "M = martensite" and "PDP = partially dissolved pearlite".

Fig. 12 reveals that a remarkable improvement in the ultimate tensile strength (UTS ~ 610 MPa) along with good ductility (percent elongation ~35%) was obtained in the annealed specimen as compared to the as-received steel. Further, continuous yielding behavior of the tensile curve (a desirable property of dual phase steels), could be achieved with such a short annealing cycle.

6. Conclusions

- The simulations could establish correctly the isothermal annealing time required for complete dissolution of pearlite into austenite under different heating rate-annealing temperature conditions. This is important for continuous annealing processes which run at very

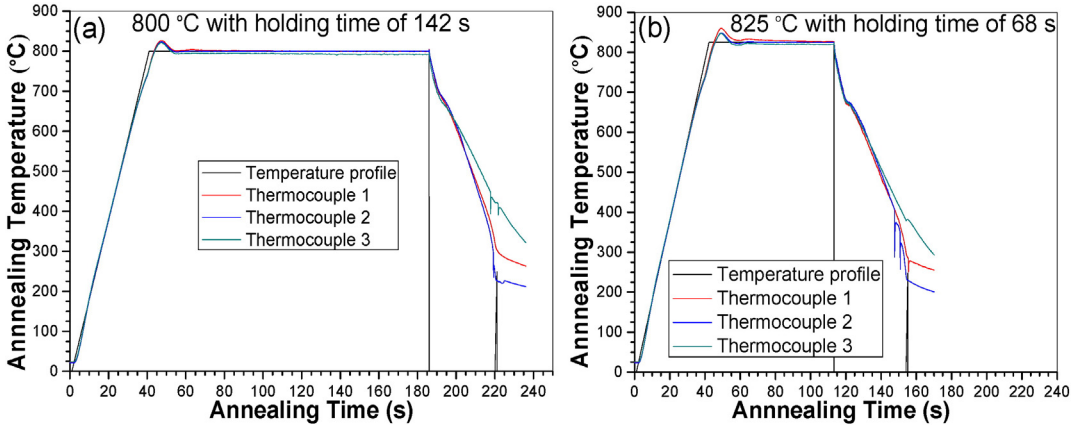

Fig. 9. Time-temperature profiles of specimens obtained from Gleeble experiments for heating rate of 20 °C/s subjected to annealing temperatures of (a) 800 °C with holding time of 142 s, and (b) 825 °C with holding time of 68 s.

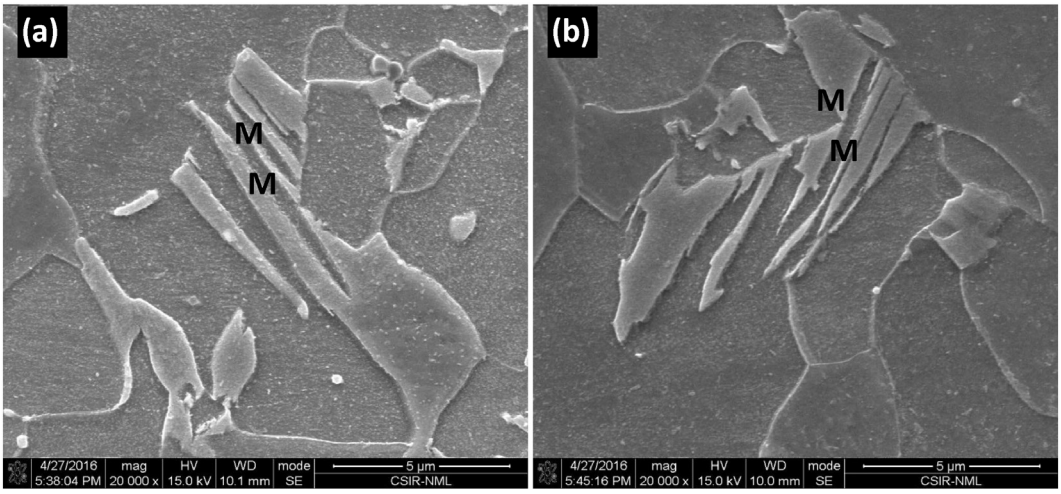

Fig. 10. FEG-SEM micrographs of specimens for heating rate of 20 °C/s subjected to annealing temperatures of (a) 800 °C with holding time of 142 s, and (b) 825 °C with holding time of 68 s showing complete pearlite dissolution. Martensite lath packets are identified with 'M'.

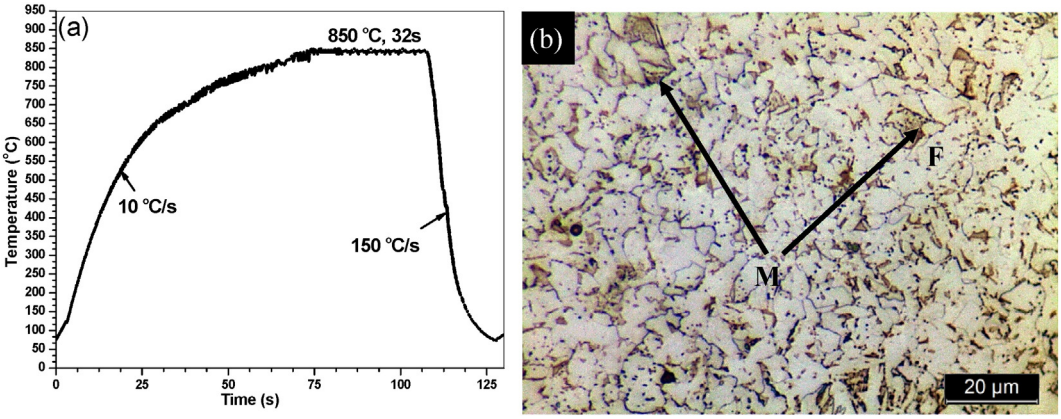

Fig. 11. (a) Time-temperature profile, and (b) typical color micrograph showing dual phase structure in the steel at annealing temperature of 850 °C with heating rate of 10 °C/s. M = martensite, dark brown color and F = ferrite, light brown color.

small soaking periods at the annealing temperature. The simulations could establish the effect of heating rate, annealing temperature, and holding time period on pearlite dissolution into austenite in a hot rolled steel intended for final dual phase properties.

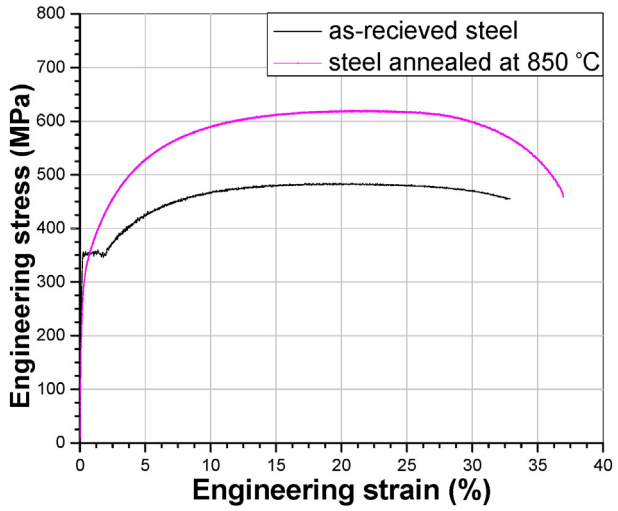

Fig. 12. Engineering stress-strain curves for the as-received steel and the specimen annealed at 850 °C.

- In the absence of soaking periods at the annealing temperature (Phase-I simulations; when only heating was considered at a particular heating rate with no consideration of soaking at the annealing temperature), simulation results showed that for a given annealing temperature, austenite fraction obtained during heating was dependent upon the heating rate. As the heating rate increased for a given annealing temperature, the austenite fraction decreased. Further, for a given heating rate, with increase in temperature, the amount of pearlite dissolution to austenite also increased.
- Simulations results also predicted that irrespective of the heating rate followed for a given annealing temperature (Phase-II simulations), the isothermal annealing time required for just complete pearlite dissolution was approximately the same. Further, for a given heating rate, with increase in annealing temperature, the holding time required for complete pearlite dissolution decreased.
- The experimental investigations provided evidence that dual phase microstructure containing carbon rich martensite obtained as a result of just pearlite dissolution into austenite results in significantly improved strength-ductility combination in a hot rolled low carbon steel. Annealing at 850 °C showed a tensile property of 610 MPa with 35% elongation.

References

[1] Q. Meng, J. Li, J. Wang, Z. Zhang, L. Zhang, Effect of water quenching process on microstructure and tensile properties of low alloy cold rolled dual-phase steel, Mater. Des. 30 (2009) 2379–2385, http://dx.doi.org/10.1016/j.matdes.2008.10.026.

[2] Q. Meng, J. Li, H. Zheng, High-efficiency fast-heating annealing of a cold-rolled dual-phase steel, Mater. Des. 58 (2014) 194–197.
[3] H.Y. Yu, J.Y. Shen, Evolution of mechanical properties for a dual-phase steel subjected to different loading paths, Mater. Des. 63 (2014) 412–418, http://dx.doi.org/10.1016/j.matdes.2014.06.003.
[4] N. Saeidi, F. Ashrafizadeh, B. Niroumand, F. Barlat, EBSD study of micromechanisms involved in high deformation ability of DP steels, Mater. Des. 87 (2015) 130–137, http://dx.doi.org/10.1016/j.matdes.2015.07.134.
[5] F. Zhang, A. Ruimi, P.C. Wo, D.P. Field, Morphology and distribution of martensite in dual phase (DP980) steel and its relation to the multiscale mechanical behavior, Mater. Sci. Eng. A 659 (2016) 93–103, http://dx.doi.org/10.1016/j.msea.2016.02.048.
[6] Z.P. Xiong, A.G. Kostryzhev, N.E. Stanford, E.V. Pereloma, Microstructures and mechanical properties of DP and TRIP steels after laboratory simulated strip casting, Mater. Des. 88 (2015) 537–549.
[7] S.A. Etesami, M.H. Enayati, A. Taherizadeh, B. Sadeghian, The Influence of Volume Fraction of Martensite and Ferrite Grain Size on Ultimate Tensile Strength and Maximum Uniform True Strain of Dual Phase Steel, Trans. Indian Inst. Metals, 2016, http://dx.doi.org/10.1007/s12666-015-0739-x.
[8] X. Cornet, J.C. Herman, Method for Making a Multiphase Hot-Rolled Steel Strip, US 2003/0041933 A1, 2003.
[9] W. Srijampan, A. Wiengmoon, M. Morakotjinda, R. Krataitong, T. Yotkaew, N. Tosangthum, et al., Microstructure and mechanical property of sintered Fe-Cr-Mo steels due to phase transformations with fast cooling rates, Mater. Des. 88 (2015) 693–701, http://dx.doi.org/10.1016/j.matdes.2015.09.030.
[10] A. Wrożyna, M. Pernach, R. Kuziak, M. Pietrzyk, Experimental and numerical simulations of phase transformations occurring during continuous annealing of DP steel strips, J. Mater. Eng. Perform. (2016), http://dx.doi.org/10.1007/s11665-016-1907-9.
[11] R. Kuziak, R. Kawalla, S. Waengler, Advanced high strength steels for automotive industry, Arch. Civ. Mech. Eng. 8 (2008) 103–117, http://dx.doi.org/10.1016/S1644-9665(12)60197-6.
[12] S. Sodjit, V. Uthaisangsuk, Microstructure based prediction of strain hardening behavior of dual phase steels, Mater. Des. 41 (2012) 370–379, http://dx.doi.org/10.1016/j.matdes.2012.05.010.
[13] S.K. Paul, Real microstructure based micromechanical model to simulate microstructural level deformation behavior and failure initiation in DP 590 steel, Mater. Des. 44 (2013) 397–406, http://dx.doi.org/10.1016/j.matdes.2012.08.023.
[14] W. Wang, X. Wei, The effect of martensite volume and distribution on shear fracture propagation of 600-1000 MPa dual phase sheet steels in the process of deep drawing, Int. J. Mech. Sci. 67 (2013) 100–107, http://dx.doi.org/10.1016/j.ijmecsci.2012.12.011.
[15] A. Imandoust, A. Zarei-Hanzaki, S. Heshmati-Manesh, S. Moemeni, P. Changizian, Effects of ferrite volume fraction on the tensile deformation characteristics of dual phase twinning induced plasticity steel, Mater. Des. 53 (2014) 99–105, http://dx.doi.org/10.1016/j.matdes.2013.06.033.
[16] J.E. Garcia-gonzalez, Fundamental Study of the Austenite Formation and Decomposition in Low-Si, Al Added Trip Steels, University of Pittsburgh, 2005.
[17] A.I. Katsamas, A computational study of austenite formation kinetics in rapidly heated steels, Surf. Coat. Technol. 201 (2007) 6414–6422, http://dx.doi.org/10.1016/j.surfcoat.2006.12.014.
[18] M.G. Mecozzi, C. Bos, J. Sietsma, A mixed-mode model for the ferrite-to-austenite transformation in a ferrite/pearlite microstructure, Acta Mater. 88 (2015) 302–313, http://dx.doi.org/10.1016/j.actamat.2015.01.058.
[19] G.R. Speich, V.a. Demarest, R.L. Miller, Formation of austenite during intercritical annealing of dual-phase steels, Metall. Trans. A 12 (1981) 1419–1428, http://dx.doi.org/10.1007/BF02643686.
[20] Y.-B. Cho, The Kinetics of Austenite Formation during Continuous Heating of a Multi-Phase Steel, The University of British Columbia, 2000.
[21] F.L.G. Oliveira, M.S. Andrade, A.B. Cota, Kinetics of austenite formation during continuous heating in a low carbon steel, Mater. Charact. 58 (2007) 256–261, http://dx.doi.org/10.1016/j.matchar.2006.04.027.
[22] M. Enomoto, K. Hayashi, Simulation of the growth of austenite during continuous heating in low carbon iron alloys, J. Mater. Sci. 50 (2015) 6786–6793, http://dx.doi.org/10.1007/s10853-015-9234-3.
[23] Y. Mazaheri, A. Kermanpur, A. Najafizadeh, A.G. Kalashami, Kinetics of ferrite recrystallization and austenite formation during intercritical annealing of the cold-rolled ferrite/martensite duplex structures, Metall. Mater. Trans. A 47 (2016) 1040–1051, http://dx.doi.org/10.1007/s11661-015-3288-3.
[24] P. Li, J. Li, Q. Meng, W. Hu, D. Xu, Effect of heating rate on ferrite recrystallization and austenite formation of cold-roll dual phase steel, J. Alloys Compd. 578 (2013) 320–327, http://dx.doi.org/10.1016/j.jallcom.2013.05.226.
[25] P. Wycliffe, Austenite Growth in Intercritical Annealing of Dual Phase Steels, McMaster University, 1982.
[26] H. Chen, X. Xu, W. Xu, S. Van Der Zwaag, Predicting the austenite fraction after intercritical annealing in lean steels as a function of the initial microstructure, Metall. Mater. Trans. A Phys. Metall. Mater. Sci. 45 (2014) 1675–1679, http://dx.doi.org/10.1007/s11661-014-2186-4.
[27] W.D. Callister, Materials Science and Engineering: An Introduction, nineth ed., 2014, http://dx.doi.org/10.1016/0261-3069(91)90101-9.
[28] S.H. Avner, Introduction to Physical Metallurgy, second ed. Tata McGraw Hill, New Delhi, 2005.
[29] R. Abbaschian, L. Abbaschian, R.E.R. Hill, Physical Metallurgy Principles, fourth ed. Cengage Learning, Stamford, 2009.
[30] N. Fonstein, Advanced High Strength Sheet Steels Physical Metallurgy, Design, Processing, and Properties, Springer International Publishing, Switzerland, 2015, http://dx.doi.org/10.1007/978-3-319-19165-2.